Journal of Hazardous Materials 384 (2020) 121272

Contents lists available at ScienceDirect

Journal of Hazardous Materials

journal homepage: www.elsevier.com/locate/jhazmat

Magnetic biochar derived from biosolids via hydrothermal carbonization: Enzyme immobilization, immobilized-enzyme kinetics, environmental toxicity

He Zhang[a,b], Anthony G. Hay[b,*]

[a] College of environmental science and technology, Donghua University, Shanghai, 201620, PR China
[b] Department of Microbiology, Cornell University, Ithaca, NY 14853, USA

GRAPHICAL ABSTRACT

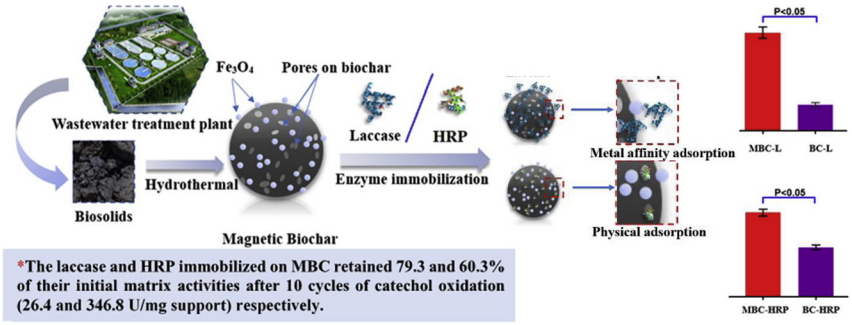

ARTICLE INFO

Editor: Daniel CW Tsang

Keywords:
Waste recycling
Biocatalysis
Sewage sludge

ABSTRACT

Magnetic and nonmagnetic biochar (MBC & BC) were produced from biosolids under hydrothermal conditions and characterized in order to understand surface chemistry impacts on enzyme immobilization and activity. Peak surface pore size of MBC was 180 nm and that of BC was 17 nm. Despite similar surface area (≈ 49 m^2/g) MBC immobilized more laccase (99 mg/g) than biochar (31 mg/g). For horseradish peroxidase (HRP), the two biochars had similar immobilization capacity (≈ 65 mg/g). Laccase and HRP on MBC had 47.1 and 18.0% higher specific activity than on BC, respectively. The matrix activity of MBC-laccase (33.3 U/mg support) was 3.7-fold higher than BC-laccase (8.8 U/mg support) and higher than the same amount of free laccase (30.2 U) at pH 3.0 ($P < 0.05$). Although MBC had its own peroxide oxidation activity (104.1 and 165.9 U/mg biochar at pHs 5&6) this only accounted for 16.7 and 20.4% of the total MBC-H RP activity respectively. After 10 wash cycles, MBC still retained 79.3% and 60.3% of laccase and HRP activity, respectively. Additionally, MBC had lower acute toxicity, suggesting that it is relative benign from an environmental perspective.

1. Introduction

Immobilization of enzymes can increase their stability and reusability. Several enzyme immobilization methods have been designed based on physical, covalent, or affinity interactions (Hosseini et al., 2018; Huang et al., 2018; Zang et al., 2014). A large number of inorganic and organic materials have been evaluated as immobilization matrices (Coradi et al., 2018; Maksym et al., 2017; Patel et al., 2017;

* Corresponding author.
E-mail address: agh5@cornell.edu (A.G. Hay).

https://doi.org/10.1016/j.jhazmat.2019.121272
Received 2 May 2019; Received in revised form 11 September 2019; Accepted 20 September 2019
Available online 21 September 2019

Wang et al., 2010). Among these, carbon-based materials are gaining increased attention for their potential to improve immobilization efficiency and their environmental friendly nature (Patel et al., 2017; Rani et al., 2000; Ye et al., 2019, 2017). For instance, Rani et al. used a charcoal-immobilized enzymes for starch hydrolysis that retained over 90% of the free enzyme's catalytic activity (Rani et al., 2000). Patel et al. reported composites synthesized from reduced graphene oxide and magnetic materials as supports for enzyme immobilization and found immobilized enzymes exhibited excellent activity with low acute toxicity toward *Vibrio fischeri* (Patel et al., 2017). Magnetic nanoparticles have also previously been shown to be efficient enzyme supports that enhanced the activity of some immobilized enzymes and could easily be recycled, but like many other enzyme support matrices, often require expensive chemicals for their synthesis which has limited widespread application of magnetic nanoparticles (Patel et al., 2017; Wu et al., 2018). Additionally, some support materials can inhibit the activity of immobilized enzymes, leading to the deceleration of enzymatic activity (Costa et al., 2019).

Magnetic biochar (MBC) derived from waste is an attractive alternative material for enzyme immobilization due to its low cost, readily available starting materials, and lack of enzyme inhibition. The porous nature of MBC contributes to its loading capacity and attractiveness as a solid support matrix (Sun et al., 2019). Furthermore, the heterogenous iron and porous carbon nature contribute to the multifunctionality of MBC (i.e., adsorption and catalytic reaction etc.) (Cho et al., 2019).

Recently, biosolids from a wastewater treatment plant were used to synthesize magnetic biochar under simple hydrothermal conditions (Zhang et al., 2018). When that MBC was used to treat actual dyeing wastewater through a Fenton process, the chemical oxygen demand (COD) and total organic carbon (TOC) removal efficiencies reached 47 ± 3.3% and 49 ± 2.7%, respectively (Zhang et al., 2018). That MBC, containing iron oxide, was shown to be an effective catalyst, converting H_2O_2 to hydroxyl radical although the rates of catalysis were low (≈26%) compared to rates reported for immobilized enzymes (Zhang et al., 2018).

Hydrothermal treatment (HT) is an efficient thermal technology that can convert waste biomass to biochar (BC) (Zhang et al., 2018). HT offers several advantages over pyrolysis and other thermal technologies, because it requires relatively low temperatures 180–250 ℃ and works on high moisture substrates like biosolids and agricultural waste without requiring them to be dried first (Zhang et al., 2018). In addition to having catalytic properties of its own, MBC also offers the advantage of being easily separated and recycled from reactions, making it an attractive means of extending the longevity of expensive enzymes.

Laccase and horseradish peroxidase (HRP) are the most common industrial enzymes used in model systems for immobilization studies (Bilal et al., 2018; Ma et al., 2018; Patel et al., 2017; Sun et al., 2018; Wu et al., 2018). Laccase can oxidize a wide range of aromatic and non-aromatic compounds including phenols (Rangelov and Nicell, 2018), and a variety of non-phenolic compounds (Ázar et al., 2018; Yesilada et al., 2018). HRP has also been widely used in biomedical, environmental, and industrial biotechnology applications (Forgiarini and de Souza, 2007). Therefore, these two enzymes were also chosen in this study.

Using a new batch of MBC from a different source of biosolids, but synthesized under hydrothermal conditions as described previously (Zhang et al., 2018), the aim of this work was to test this MBC's utility as a support matrix for enzyme immobilization. For comparison's sake, BC produced from the same initial biosolids material was used as a reference. Both of these newly synthesized biochars (BC and MBC) were used as supports for immobilization of laccase and HRP and evaluated using catechol as a model substrate. The mechanism of enzyme immobilization was also explored. Additionally, the toxicity of the biochars was measured to evaluate any potential environmental health concerns.

2. Experimental section

2.1. Materials and chemicals

Biosolids from the dewatering unit of the wastewater treatment plant in Ithaca, New York (USA), were collected for this study. Basic information about the wastewater treatment facility is in the supplementary information (SI). The biosolids were immediately transferred to the laboratory and stored at 4 ℃ prior to use. Laccase (*Trametes versicolor*, EC: 1.10.3.2) and horseradish peroxidase (HRP EC: 1.11.1.7) were purchased from Sigma-Aldrich (USA). All other chemicals and reagents used in the experiments were analytical grade from commercial sources and used without any further purification.

2.2. The synthesis of biochar and magnetic biochar

Magnetic biochar (MBC) was synthesized as described previously (Zhang et al., 2018). Briefly, 0.78 g $Fe_2(SO_4)_3$, 0.54 g glucose and 20 g biosolids (6 g dry weight) were combined with ultrapure water to a final volume of 80 mL. Glucose is a reducing sugar, it was added to ensure that the iron oxide in MBC was Fe_3O_4 and not Fe_2O_3. Before the HT process, the mixture was stirred (600 rpm) for 30 min and its pH was adjusted to 11 with NaOH. It was then transferred to a 100 mL Teflon reactor (PPL100, Yanzheng Co., Ltd.), sealed, and autoclaved at 180 ℃ (1 MPa) for 6 h before being allowed to cool naturally. The resultant MBC was collected by vacuum filtration (50 mm, Bio-rad) with filter paper (3 μm, Grade 6 Whatman), washed with ethanol (60 mL) and then with distilled water (60 mL) before being dried for 24 h at 40 ℃. For non-magnetic biochar (BC), the same process was followed except that the iron and glucose were omitted.

2.3. Characterization of samples

The biochars were characterized by X-ray diff ;raction (XRD) and scanning electron microscopy (SEM). The specific surface area and pore diameter distribution of samples were determined using N_2 adsorption-desorption isotherms and were calculated by the Brunauer-Emmett-Teller (BET) and Barrett-Joyner-Halenda (BJH) methods (Brunauer et al., 1938), respectively. The functional groups were characterized by Fourier transform infrared spectroscopy (FT-IR). The hysteresis curve of MBC was obtained by vibrating sample magnetometry (VSM), surface elements composition was measured by an energy dispersive spectrometer (EDS), the valence states of iron were analyzed by X-ray photoelectron spectroscopy (XPS). High Performance Liquid Chromatography (HPLC) was used to measure the catechol concentration in solution. Details are shown in the SI.

2.4. Enzyme immobilization

Enzyme immobilization on BC and MBC was tested at various pH values using Na_2HPO_4-Citric acid buffers (0.2 M, pH 2.0–7.0). The biochars (10 mg) were mixed with enzymes (1 mg protein) in 1 mL of buffered solution with different pH values and incubated for 1.5 h with shaking at 900 rpm at 4 ℃. After the adsorption of enzymes, the biochars were separated by centrifugation at 9600 × g for 15 min. The same pH buffer was used to wash the enzyme-laden biochars three times. The protein concentration of the supernatant was measured by the Bradford method (Bradford, 1976) and the biochar loading was calculated by subtraction from the no-biochar controls.

2.5. The activity of free and immobilized enzyme

The activity assay of the free and immobilized laccase and HRP were determined spectrophotometrically (λ = 410 nm) in a reaction medium containing 0.1% (w/v) catechol as substrate at 25 ℃ in buffers (pH 3.0) and (pH 7.0), respectively. Catechol is a widely used substrate for

measuring the activity of laccases and oxidases (Durán et al., 2002) and because it can undergo redox cycling it can potentially inactive enzymes attempting to degrade it, thus the ability to degrade catechol sets a high bar for enzyme stability. Enzyme-immobilized biochars (2.5 mg) were added to 1 mL of the 0.1% catechol solution. Free enzyme (equal in concentration for that calculated to be on the biochar) was added to the substrate solution and shaken at 900 rpm for 10 min. Change in the absorbance of the supernatant of replicate samples was determined in a 96 well microplate reader (Synergy HT, BioTek). The molar absorption coefficient (2211 $M^{-1}\,cm^{-1}$) of catechol in our buffer system was calculated from the HPLC results. Enzyme activities were expressed as international units (IU), where one IU represents the amount of enzyme that forms $\mu mol{\cdot}min^{-1}$ products under standard assay conditions. Activity of immobilized enzymes was reported per gram of matrix (matrix activity) for easier comparison between BC and MBC because of their different enzyme loading rates.

2.6. Kinetic parameters and properties of enzyme

Kinetic parameters of Michaelis–Menten equation (K_m and K_{cat}) for free and immobilized enzymes were determined by measuring initial rates of the reaction with catechol (0.01–5 mM for Laccase, 0.01–10 mM for HRP) at constant temperature and pH. The kinetic constants (K_m and K_{cat}) were obtained by using enzyme kinetics function in GraphPad Prism 6.

2.7. Reusability of immobilized enzyme

Enzyme reusability was investigated by recovering the immobilized laccase or HRP via either centrifugation (BC) or magnetic capture (MBC) and resuspending them in new reaction buffer as described previously for MBC (Zhang et al., 2018). Each round of the reaction was performed at 25 °C under standard assay conditions mentioned above and compared to a free enzyme control.

2.8. Toxicity analysis

The acute toxicity of the MBC and BC were assessed using a luminescent bacteria toxicity test according to ISO 11348-1 (ISO, 11348-1:, 2007). Briefly, MBC and BC (10 mg/mL) were prepared in distilled water containing 2% NaCl solution. Cells of the luminescent marine bacterium *Vibrio fischeri* (100 µl, OD600 = 2) were added to an equal volume of the biochar suspension in a 96-well microplate and luminescence was measured after 15 and 30 min in the Synergy HT plate reader. The impact of the biochar on luminescence was reported as the $EC_{50-15min}$ and $EC_{50-30min}$ respectively, which denote the effective concentration (EC) of the suspension that caused a 50% reduction in the luminescence of the bacteria after incubation for the indicated time. Triclosan, a widely-available antimicrobial compound, was used as a control toxicant to permit future comparisons with materials from other laboratories where bacterial strain and experimental differences might otherwise prevent meaningful comparisons.

3. Results and discussion

3.1. Synthesis and characterization of biochars

As shown in Fig. 1, the XRD pattern of MBC showed diffraction peaks at 2θ = 30.1°, 35.5°, 43.1°, 53.5°, 56.9° and 62.6°, which were assigned to the (220), (311), (400), (422), (511) and (440) planes of Fe_3O_4 respectively and are consistent with the observed magnetic characteristics. Hematite and magnetite, however, have similar XRD spectra, thus XPS analysis was performed to confirm the presence of magnetite. The XPS spectra of Fe(2p) and the deconvoluted spectra of Fe(2p) of MBC are shown in Fig. 1B. There is no satellite peak at 719 eV, and the deconvoluted area of Fe^{2+} and Fe^{3+} is around 1:2, thus the iron oxide is magnetite (Fe_3O_4) instead of hematite (Fe_2O_3) (Fujii et al., 1999). The sole peak of BC was noted at 2θ = 26.4°, corresponding to typical crystalline SiO_2. These data demonstrate magnetite is the main iron oxide in MBC and that HT of biosolids alone did not produce a magnetic compound. The pore size distribution curves for BC and MBC are in Fig. 2A. The hysteresis loop of BC revealed that mesopores with a pore diameter of 20–50 nm were present, but that average pore size was 17 nm. It is likely that the actual surficial openings in BC were less than 17 nm given the non-uniform and hierarchical porous structure that was evident in the SEM images. That contrasted significantly with the pore diameter of MBC which ranged from 50 to more than 500 nm, with an average pore size around 180 nm. This suggests that the iron oxide increased the size of biochar pores. In a related study, iron increased the pore size of biosolids-derived biochar by hydrothermal carbonization, though the mechanism remains unknown (Cai et al., 2019). In addition, the isotherms of MBC and BC (Fig. 2b) both fell within IUPAC classification type III (Zhou et al., 2015), showing that adsorption equilibrium was not reached even at high relative pressures. Even though MBC pores were larger than those of BC, both had the similar specific surface area (S_{BET}, 48.55 m^2/g for MBC versus S_{BET}, 48.59 m^2/g for BC).

The surface morphologies of BC and MBC are shown in Fig. 3A and B. The BC exhibited a bulky structure with a globular and porous surface. In the case of MBC, the SEM images showed that most particles had a flaky, somewhat columnar structure.

3.2. Enzyme immobilization and kinetics

Laccase loading on BC and MBC were dependent on pH and reached its maximum at pH 3 (Fig. 4). The *T. versicolor* laccase used in this work has an isoelectric point (pI) of about pH 3 (Piontek et al., 2002), thus the surface of laccase was positively charged below pH 3 and became progressively negatively charged above pH 3. The amount of laccase immobilized on biochar was 31 mg/g·BC at pH 3. The approximate diameter of laccase is around 18.5 nm (Bertrand et al., 2002), which was larger than the average pore size of BC (17 nm), which suggests that this small pore size might have been one factor limiting laccase loading on BC. The portion of laccase that was immobilized on BC (31%) was likely retained in less abundant large pores that ranged up to 50 nm. In contrast, laccase immobilization of MBC reached almost 98 mg/g MBC at the optimal pH. It is speculated, that this greater immobilization was due, not only to more accommodating pore size, but also because metal affinity adsorption was present in MBC, but not BC.

Based on the Lewis-acid/base concepts of Pearson (Pearson, 1968), iron ions on the surface of MBC are expected to act as soft or borderline Lewis acids, exhibiting a preference for non-bonding lone pair electrons from nitrogen atoms in aromatic and aliphatic amino containing ligands (Wang et al., 2008). This is hypothesized to result in affinity between exposed side chains of Laccase amino acids (i.e. especially imidazole groups of the histidine residues) and iron ions (Wang et al., 2008). A similar observation of metal affinity was reported previously regarding glucoamylase immobilization by magnetic particles (Wang et al., 2007) and is supported by the FTIR measurements discussed below.

Both biochars performed similarly for HRP immobilization, retaining 65 mg/g·BC and 68 mg/g·MBC at pH 6. The approximate diameter of HRP is around 14 nm (Gajhede et al., 1997), which is smaller than the average surface pore size of either biochar, thus it is not surprising that both BC and MBC had similar adsorption of HRP. The HRP immobilization efficiency decreased gradually as pH increased. Although the pI of HRP is about pH 8, the enzyme immobilized efficiently onto BC and MBC, reaching its maximum value at pH 2. Based on their zeta potentials at different pHs (Figure S4), the zero point of charge (pH_{zpc}) of BC and MBC are 2.39 and 1.62, respectively. When the pH of solution is 2, the surface charge of two biochars approach the minimum, resulting in the high HRP immobilization efficiency.

Although both enzymes were immobilized onto BC and MBC successfully, the mechanism behind their adsorption required further

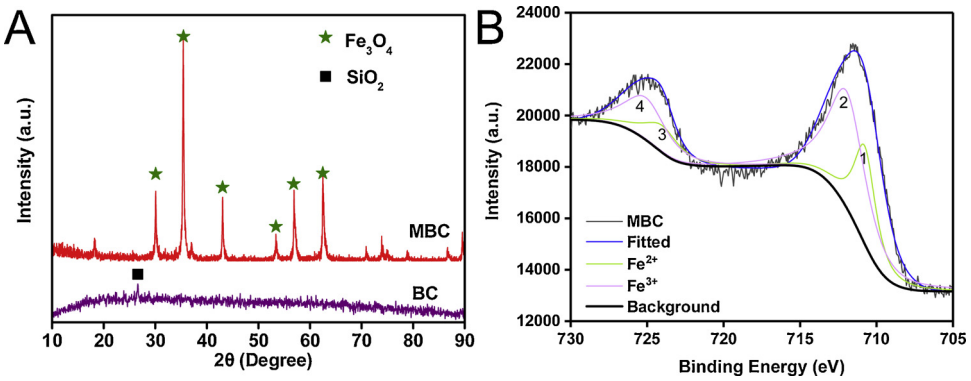

Fig. 1. A) XRD patterns of MBC and BC; B) XPS spectra of Fe(2p) and the deconvoluted spectra of Fe(2p) of MBC (The area of peaks: 1- 9480; 2- 18854; 3- 4161; 4- 8037).

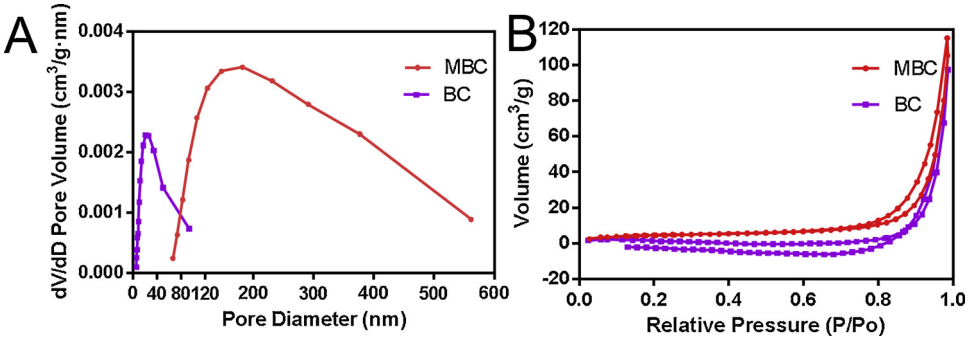

Fig. 2. Characterization of biochars by N_2 adsorption-desorption: (A) pore size distribution; (B) adsorption-desorption isotherms.

investigation. FTIR has been widely used to examine the chemical changes occurring during the immobilization of enzymes and was therefore employed to better understand the mechanism behind our observations (Patel et al., 2017). As shown in Fig. 5A, the spectra revealed the nature of numerous chemical bonds for MBC, BC, enzymes and both biochars loaded with each enzyme. These included the C—H stretching vibrations of the CH, and CH_3 groups (2959 and 2925 cm^{-1}) and symmetrical deformations of C—H (1448 cm^{-1}) (Schmitt and Flemming, 1998). The presence of Si-O stretching at 1031 cm^{-1} and 799 cm^{-1} was evident in both biochars. MBC-immobilized laccase (MBC-L) had an additional C═O stretching at 1700 cm^{-1} when compared with its immobilization on BC (Fig. 5B). The iron on the surface of MBC may form a dative bond with a Lewis acid (i.e. laccase) to form a Lewis adduct, resulting in the new peak at 1700 cm^{-1} in the FTIR spectrum. Patel et al. demonstrated that similar shifts were due to metal affinity adsorption of laccase to magnetic graphene oxide particles (Patel et al., 2017). This contrasted with the results for HRP immobilization which likely occurred via physical adsorption since no new peaks were found in HRP-immobilized to either biochar (Fig. 5C).

Efficient immobilization on a matrix requires not only retention of the enzyme, but also maintenance of enzyme activity after immobilization. The matrix activities of free and immobilized enzymes at different pH values are shown in Fig. 6. The activity of free and immobilized laccase on MBC (MBC-L) and BC (BC-L) was highest at pH 3.0, then decreased between pH 4-7. The matrix activity of MBC-L (33.3 U/mg support) was 3.7-fold higher than that of BC-L (8.8 U/mg support) and also significantly higher than same amount of free laccase activity (30.2 U) under pH 3.0 ($P < 0.05$). As shown in Figure S5, the activity of free laccase, MBC-L, and BC-L was highest at pH 3.0, but changed little between pH 4-7. The specific activity of MBC-L (3.2×10^3 U/mg protein) was higher than that of the free enzyme (2.9×10^3 U/mg protein) ($P < 0.05$). The specific activity of free laccase, however, was not significantly different than that of the BC-L (2.8×10^3 U/mg protein, $P > 0.05$).

The activities of free and immobilized HRP were sensitive to pH change and reached a maximum at pH 6 (Fig. 6B). The matrix activity

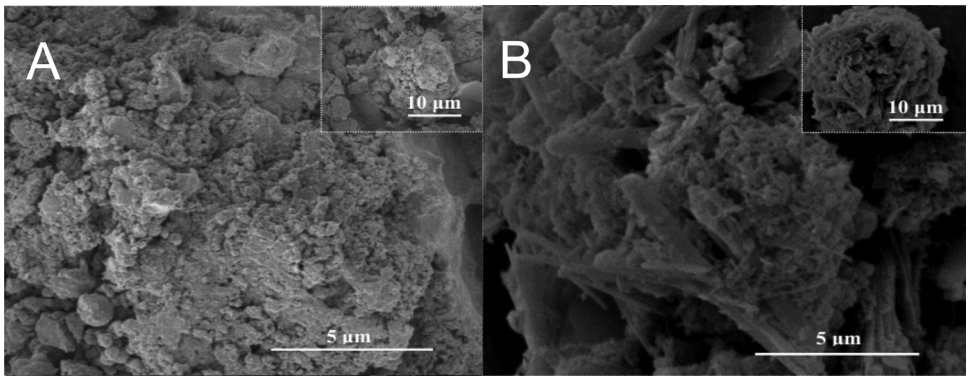

Fig. 3. The SEM image of the synthesized A) BC, B) MBC.

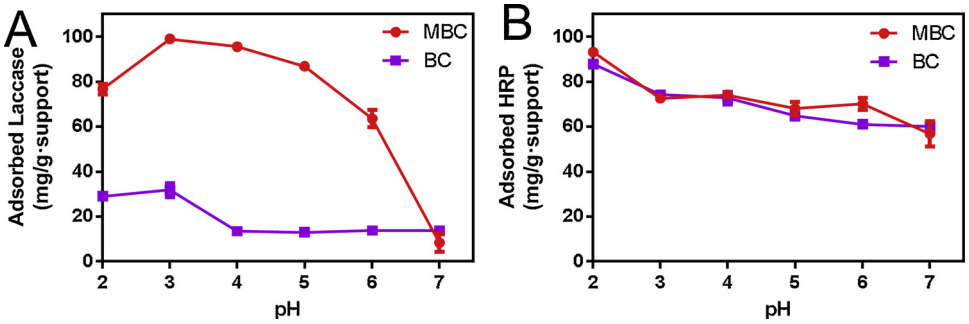

Fig. 4. Effect of pH on Enzyme immobilization onto MBC and BC: (A) Laccase, (B) HRP. To determine the optimal pH value of free and immobilized enzyme, the reaction was performed under standard conditions in Na_2HPO_4-Citric acid buffer (pH 2–7).

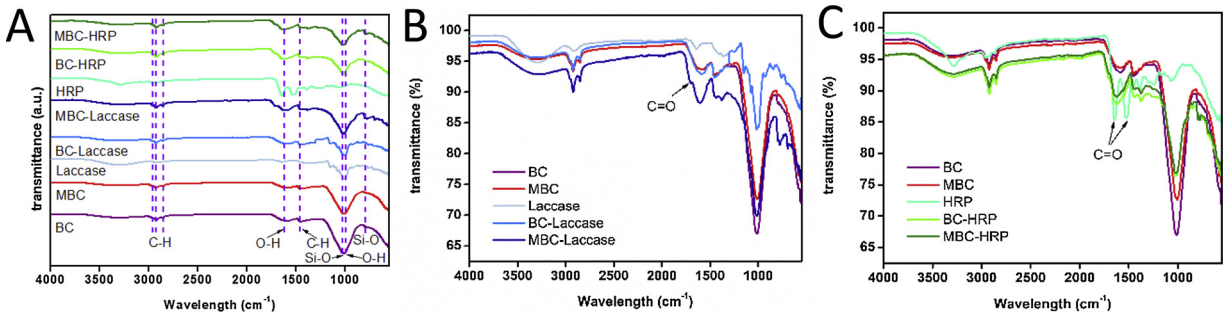

Fig. 5. Aggregated individual FT-IR spectra of MBC, BC, enzymes and enzyme-immobilized supports (A). Overlays of sprectra for (B) laccase and (C) HRP with and without MBC and BC.

of immobilized HRP on MBC (574.7 U/mg support) was higher than that of the free enzyme (462.7 U) and immobilized HRP on BC (338.2 U/mg support). Our data suggests that BC had a mild inhibitory effect on HRP specific activity. The simplest explanation for this modest effect may be mass transfer limitations between substrate and HRP caused by physical rather than affinity immobilization. In contrast, the matrix activity of HRP immobilized on MBC increased significantly when compared to either free enzyme or that immobilize on BC. The matrix activity of immobilized HRP on MBC was also significantly higher ($P < 0.05$) than free HRP incubated in the presence of MBC (added in the same tube, but not immobilized).

Peroxidase activity has been reported for large magnetite nanoparticles even in the absence of enzymes (Zhang et al., 2018). Limited peroxidase-like activity was detected in MBC without enzyme, but none in BC. Thus, the magnetite in MBC contributed directly to the observed increase in matrix activity and may also have facilitated electron transfer during the enzymatic reaction (Liu et al., 2015). The iron in MBC may also favor the formation of environmentally persistent free radicals by obtaining unpaired electrons from dissolved organic matter on biochar to oxidize the substrate (Ruan et al., 2019). These results demonstrate that MBC was more effective than BC at retaining high enzyme activity of both laccase and HRP after immobilization.

The V_{max} of the laccase on MBC (44 $\mu M \cdot Min^{-1}$) was similar to that of free laccase (43 $\mu M \cdot Min^{-1}$), and higher than when it was immobilized on BC (38 $\mu M \cdot Min^{-1}$), indicating MBC did not constrain laccase activity (Table 1). The K_m for the MBC-immobilized laccase (0.96 mM) increased compared to that of free laccase (0.72 mM). Patel et al. have demonstrated that Fe_3O_4 which is found in MBC, has a low affinity for the test substrate ABTS (Patel et al., 2017). MBC alone had a significantly lower affinity for the catechol used as a substrate (Table 1). The apparent Vmax of HRP was higher on MBC (1.5 $mM \cdot Min^{-1}$) than that of the free enzyme (1.3 $mM \cdot Min^{-1}$), whereas it decreased significantly on BC to 0.57 $mM \cdot Min^{-1}$. As with laccase, the K_m for HRP also increased when immobilized on MBC. This is consistent with the lower affinity of the Fe_3O_4 in MBC for catechol.

The catalytic efficiency (K_{cat}/K_m) of free laccase (0.074 $Min^{-1}\,mM^{-1}$) decreased when immobilized on MBC (0.059 $Min^{-1}\,mM^{-1}$). However, the catalytic efficiency of free and MBC-bound HRP (0.39 $Min^{-1}\,mM^{-1}$ and 0.36 $Min^{-1}\,mM^{-1}$, respectively) were not significantly different. The MBC-H RP, however, had almost

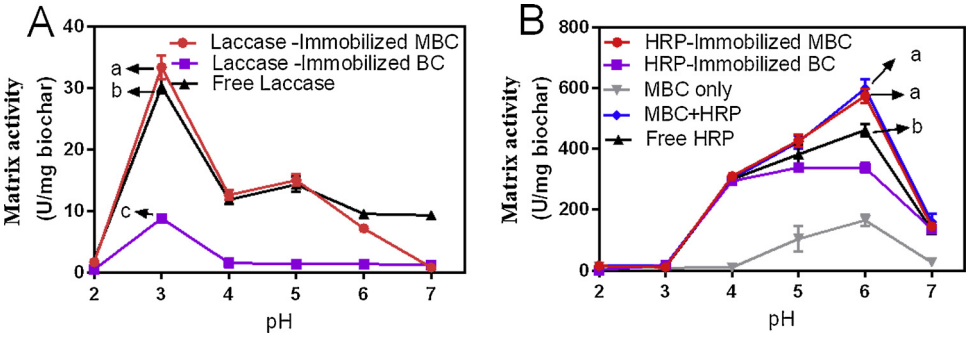

Fig. 6. Matrix activity of free enzyme and biochar-immobilized enzymes as a function of pH: (A) Laccase; (B) HRP. The amount of free enzyme was the same as the amount of enzyme immobilized on MBC (Means with same letter in each curve are not significantly different ($p < 0.05$; T-test)).

Table 1
Kinetic parameters of free and immobilized enzyme.

	Laccase			HRP				
	MBC-L	BC-L	Lac	MBC-HRP	BC-HRP	HRP	MBC + HRP*	MBC only
V_{max} ($\mu M Min^{-1}$)	[a](4.4 ± 0.3) x10	[b](3.8 ± 0.2) x10	[a](4.3 ± 0.3) x10	[a]$(1.5 \times 10^3) \pm (2.3 \times 10)$	[c]$(5.7 \times 10^3) \pm (5.3 \times 10)$	[b]$(1.3 \times 10^3) \pm (1.4 \times 10)$	[a]$(1.5 \times 10^3) \pm (3.0 \times 10)$	[d]$(0.2 \times 10^3) \pm (3.6 \times 10)$
K_m(μM)	[a](9.6 ± 1.3) x10	[b,c](7.7 ± 1.2) x10	[c](7.2 ± 1.1) x10	[c](8.0 ± 1.1) x10^3	[d](5.4 ± 0.6) x10^3	[d,e]5.2 ± 0.8 × 10^3	[a](1.0 ± 0.1)x10^4	[a,b](9.0 ± 1.0) x10^3
K_{cat}(Min^{-1})	[a](5.7 ± 0.3)x10^{-2}	[b](4.5 ± 0.2)x10^{-2}	[a](5.3 ± 0.3)x10^{-2}	[a]2.8 ± 0.2	[b]0.9 ± 0.1	[c]2.0 ± 0.1	[a]3.2 ± 0.7	[d](3.5 ± 0.4) x10^{-1}
K_{cat}/K_m ($Min^{-1}mM^{-1}$)	[a](5.9 ± 0.5)x10^{-2}	[a](5.8 ± 0.1) x10^{-2}	[b]$7.4 \times 10^{-2} \pm (6.0 \times 10^{-5})$	[a](3.6 ± 0.2) x10^{-1}	[c](1.7 ± 0.1) x10^{-1}	[a](3.9 ± 0.3) x10^{-1}	[b](3.2 ± 0.3) x10^{-1}	[d](3.8 ± 0.2) x10^{-2}

* indicates these components were added separately. Bars donate standard error of three repeats. Means with the same letter in each curve are not significantly different ($p < 0.05$; T-test).

2.0-fold higher catalytic efficiency than BC-H RP and was also significantly higher than HRP and MBC added separately in the same reaction suggesting that the Fe_3O_4 in MBC had a positive impact on HRP activity. Superparamagnetic beads have been reported to greatly enhance HRP activity though the mechanism responsible for that enhancement is distinct from the modest increases in this study (Corgié et al., 2012).

3.3. Reusability and stability of immobilized enzyme

The laccase immobilized on MBC and BC retained 79.3 and 73.9% of their initial matrix activities after 10 cycles of catechol oxidation (26.4 and 6.51 U/mg support) respectively (Fig. 7). Similarly, HRP immobilized onto MBC and BC retained 60.3 and 51.5% of their initial activities after 10 cycles of catechol oxidation, (347 and 174 U/mg support) respectively. In addition to conferring significantly higher actives after repeated use, the MBC immobilized enzymes were also much easier to recycle since magnetic separation could be used to remove them from the reaction mixture. With regards to its magnetic behavior, MBC exhibited nonlinear and reversible hysteresis (Figure S6). The saturation magnetization (Ms), remanence (Mr) and coercive force (Hc) values were 18.2 emu/g, 0.24 emu/g and 49.6 Oe, respectively.

3.4. Acute toxicity of biochars

The production of magnetic particles compatible with a broad range of biotechnological applications using environmentally friendly methods is highly desirable. The toxicity of magnetic particles is highly variable, ranging from moderately toxic to nontoxic with different model organisms or human cells (García et al., 2011). Though iron in MBC is classified as non-toxic, an increasing number of studies indicate negative impacts of iron-based particles on living organisms (Lei et al., 2018). Therefore, the toxicity of biochars was evaluated via the widely used *Vibrio fischeri* bioluminescence inhibition assay. The EC_{50} values of MBC were 1.1×10^4 and 9.9×10^3 μg/mL after 15 and 30 min of incubation, respectively (Table 2). Under similar conditions, the EC_{50} values of BC particles were 8.7×10^3 and 6.9×10^3 μg/mL, respectively. Lower $EC_{50\text{-}15min}$ and $EC_{50\text{-}30min}$ values (7.7×10^2 and 7.2×10^2 μg/mL) (Patel et al., 2017), meaning greater toxicity, were previously reported for magnetic carbon-based support materials (Patel et al., 2017). Thus, the toxicity of our MBCs was approximately 10 times lower than that reported by Patel et al. (Patel et al., 2017). Our MBC was also less toxic that other biochars made from bark and wheat straw (Gondek et al., 2017), which highlights the biocompatibility of our MBCs, thus making them an attractive option for enzyme immobilization when environmental release may occur. The toxicity of a reference standard (triclosan) was also provided, so that future work by others can be benchmarked against this widely available toxicant and lead to more reliable comparisons since biochars produced in small batches by independent academic laboratories are seldom available for comparative studies.

4. Conclusions

The MBC had a similar specific surface area (S_{BET}, 48.55 m^2/g) to BC (S_{BET}, 48.59 m^2/g) synthesized from the same biosolids, however, MBC had 10-fold bigger pores (180 nm) than BC (17 nm) which likely contributed to enhanced enzyme immobilization in the case of HRP. Metal-affinity interactions with MBC likely also contributed to the enhanced immobilization of laccase. The MBC-H RP had almost 2.0-fold higher catalytic efficiency than BC-H RP. The MBC-L and MBC-H PR retained 79.3 and 60.3% of their initial matrix activities after 10 cycles of catechol oxidation, respectively. Over all, MBC resulted in significant improvements to enzyme stability, activity, and reusability. MBC also had 10 times lower acute toxicity towards *Vibrio fischeri* than previously

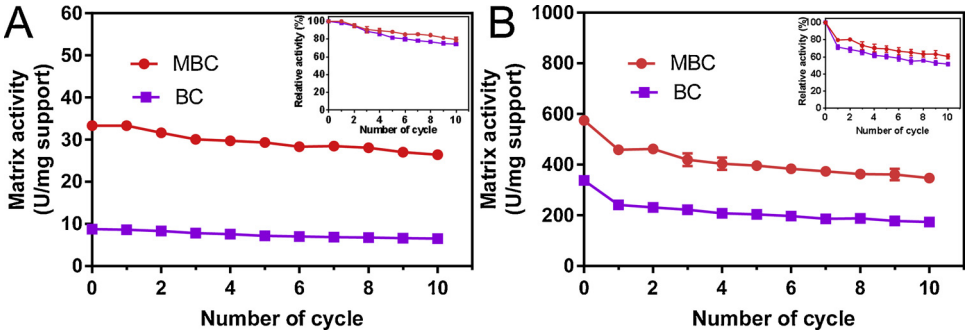

Fig. 7. Reusability and stability of immobilized enzymes: (A) Laccase; (B) HRP. Catechol disappearance was quantified via HPLC. The immobilized enzymes were washed after each cycle then resuspended in reaction buffer. Cycle times: Laccase-30 min, HRP-5 min (Error bars represent one standard deviation, n = 3). The initial matrix activity of immobilized enzyme was considered as 100% for the inserts. In all cases, the activity of both enzymes was significantly higher on MBC than on BC ($P < 0.05$).

Table 2
Acute toxicity of biochars and carbon-based materials/biochars in publication towards *Vibrio fischeri*.

Biochars		Parameter[a]	EC_{50} value (μg/mL)
MBC		$EC_{50-15min}$	[a]1.08×10^4
		$EC_{50-30min}$	[a]9.87×10^3
BC		$EC_{50-15min}$	[a]8.71×10^3
		$EC_{50-30min}$	[b]6.95×10^3
Triclosan		$EC_{50-15min}$	2.2
Fe_3O_4-reduced graphene oxide(Patel et al., 2017)		$EC_{50-15min}$	7.70×10^2
		$EC_{50-30min}$	7.20×10^2
Biochars[b](Gondek et al., 2017)	bark	$EC_{50-15min}$	49
	wheat straw		100

[a] $EC_{50-15min}$ and $EC_{50-30min}$ were determined based on the bioluminescence after 15 and 30 min of incubation, respectively and compared to a readily available standard triclosan. Means with the same letter in each curve are not significantly different ($p < 0.05$; T-test);[b]dosage of each biochar was 250 μg/mL, the EC_{50} value was presented by inhibition (%).

described carbon-based supports. The data presented herein provide strong evidence that MBC is a promisingsupport matrix for enzyme immobilization applications, making it a value-added product from unwanted waste products like biosolids.

Acknowledgements

This research was funded by China Scholarship Council (CSC) and Cornell CCMR facility grant (DMR-1719875).

Appendix A. Supplementary data

Supplementary material related to this article can be found, in the online version, at doi:https://doi.org/10.1016/j.jhazmat.2019.121272.

References

Ázar, R.I.S.L., Morgan, T., dos Santos, A.C.F., de Aquino Ximenes, E., Ladisch, M.R., Guimarães, V.M., 2018. Deactivation and activation of lignocellulose degrading enzymes in the presence of laccase. Enzyme Microb. Tech. 109, 25–30.
Bertrand, T., Jolivalt, C., Briozzo, P., Caminade, E., Joly, N., Madzak, C., Mougin, C., 2002. Crystal structure of a four-copper laccase complexed with an arylamine: insights into substrate recognition and correlation with kinetics. Biochem 41 (23), 7325–7333.
Bilal, M., Rasheed, T., Iqbal, H.M.N., Hu, H., Wang, W., Zhang, X., 2018. Horseradish peroxidase immobilization by copolymerization into cross-linked polyacrylamide gel and its dye degradation and detoxification potential. Int. J. Biol. Macromol. 113, 983–990.
Bradford, M.M., 1976. A rapid and sensitive method for the quantitation of microgram quantities of protein utilizing the principle of protein-dye binding. Anal. Biochem. 72 (1-2), 248–254.
Brunauer, S., Emmett, P.H., Teller, E., 1938. Adsorption of gases in multimolecular layers. J. Am. Chem. Soc. 60 (2), 309–319.
Cai, W., Wei, J., Li, Z., Liu, Y., Zhou, J., Han, B., 2019. Preparation of amino-functionalized magnetic biochar with excellent adsorption performance for Cr(VI) by a mild one-step hydrothermal method from peanut hull. Colloid Surf. A 563, 102–111.
Cho, D.-W., Yoon, K., Ahn, Y., Sun, Y., Tsang, D.C.W., Hou, D., Ok, Y.S., Song, H., 2019. Fabrication and environmental applications of multifunctional mixed metal-biochar composites (MMBC) from red mud and lignin wastes. J. Hazard. Mater. 374, 412–419.
Coradi, M., Zanetti, M., Valério, A., de Oliveira, D., da Silva, A., Ulson, S.Md.A.G., de Souza, A.A.U., 2018. Production of antimicrobial textiles by cotton fabric functionalization and pectinolytic enzyme immobilization. Mater. Chem. Phys. 208, 28–34.
Corgié, S.C., Kahawong, P., Duan, X., Bowser, D., Edward, J.B., Walker, L.P., Giannelis, E.P., 2012. Self-assembled complexes of horseradish peroxidase with magnetic nanoparticles showing enhanced peroxidase activity. Adv. Funct. Mater. 22 (9), 1940–1951.
Costa, J.B., Lima, M.J., Sampaio, M.J., Neves, M.C., Faria, J.L., Morales-Torres, S., Tavares, A.P.M., Silva, C.G., 2019. Enhanced biocatalytic sustainability of laccase by immobilization on functionalized carbon nanotubes/polysulfone membranes. Chem. Eng. J. 355, 974–985.
Durán, N., Rosa, M.A., D'Annibale, A., Gianfreda, L., 2002. Applications of laccases and tyrosinases (phenoloxidases) immobilized on different supports: a review. Enzyme Microb. Tech. 31 (7), 907–931.
Forgiarini, E., de Souza, A.A.U., 2007. Toxicity of textile dyes and their degradation by the enzyme horseradish peroxidase (HRP). J. Hazard. Mater. 147 (3), 1073–1078.
Fujii, T., De Groot, F.M.F., Sawatzky, G.A., Voogt, F.C., Hibma, T., Okada, K., 1999. In situ XPS analysis of various iron oxide films grown by NO_2-assisted molecular-beam epitaxy. Phy. Rev. B 59 (4), 3195.
Gajhede, M., Schuller, D.J., Henriksen, A., Smith, A.T., Poulos, T.L., 1997. Crystal structure of horseradish peroxidase C at 2.15 Å resolution. Nat. Struct. Biol. 4 (12), 1032.
García, A., Espinosa, R., Delgado, L., Casals, E., González, E., Puntes, V., Barata, C., Font, X., Sánchez, A., 2011. Acute toxicity of cerium oxide, titanium oxide and iron oxide nanoparticles using standardized tests. Desalination 269 (1-3), 136–141.
Gondek, K., Mierzwa-Hersztek, M., Baran, A., Szostek, M., Pieniążek, R., Pieniążek, M., Stanek-Tarkowska, J., Noga, T., 2017. The effect of low-temperature conversion of plant materials on the chemical composition and ecotoxicity of biochars. Waste Biomass Valori 8 (3), 599–609.
Hosseini, S.H., Hosseini, S.A., Zohreh, N., Yaghoubi, M., Pourjavadi, A., 2018. Covalent immobilization of cellulase using magnetic poly(ionic liquid) support: improvement of the enzyme activity and stability. J. Agric. Food Chem. 66 (4), 789–798.
Huang, T., Liu, Z., Li, Y., Li, Y., Chao, L., Chen, C., Tan, Y., Xie, Q., Yao, S., Wu, Y., 2018. Oxidative polymerization of 5-hydroxytryptamine to physically and chemically immobilize glucose oxidase for electrochemical biosensing. Anal. Chim. Acta 1013, 26–35.
ISO 11348-1, 2007. I. Water Quality – Determination of the Inhibitory Effect of Water Samples on the Light Emission of Vibrio fischeri (Luminescent Bacteria Test) - Part 1: Method Using Freshly Prepared Bacteria.
Lei, C., Sun, Y., Tsang, D.C.W., Lin, D., 2018. Environmental transformations and ecological effects of iron-based nanoparticles. Environ. Pollut. 232, 10–30.
Liu, F., Rotaru, A.E., Shrestha, P.M., Malvankar, N.S., Nevin, K.P., Lovley, D.R., 2015. Magnetite compensates for the lack of a pilin-associated c-type cytochrome in extracellular electron exchange. Environ. Microbiol. 17 (3), 648–655.
Ma, H.-F., Meng, G., Cui, B.-K., Si, J., Dai, Y.-C., 2018. Chitosan crosslinked with genipin as supporting matrix for biodegradation of synthetic dyes: laccase immobilization and characterization. Chem. Eng. Res. Des. 132, 664–676.
Maksym, P., Tarnacka, M., Dzienia, A., Matuszek, K., Chrobok, A., Kaminski, K., Paluch, M., 2017. Enhanced polymerization rate and conductivity of ionic liquid-based epoxy resin. Macromolecules 50 (8), 3262–3272.
Patel, S.K.S., Choi, S.H., Kang, Y.C., Lee, J.-K., 2017. Eco-friendly composite of $Fe3O_4$-reduced graphene oxide particles for efficient enzyme immobilization. ACS Appl. Mater. Interface 9 (3), 2213–2222.
Pearson, R.G., 1968. Hard and soft acids and bases, HSAB, part 1: fundamental principles. J. Chem. Educ. 45 (9), 581.
Piontek, K., Antorini, M., Choinowski, T., 2002. Crystal structure of a laccase from the fungusTrametes versicolor at 1.90-Å resolution containing a full complement of coppers. J. Biol. Chem. 277 (40), 37663–37669.
Rangelov, S., Nicell, J.A., 2018. Modelling the transient kinetics of laccase-catalyzed oxidation of four aqueous phenolic substrates at low concentrations. Biochem. Eng. J. 132, 233–243.
Rani, A.S., Das, M.L.M., Satyanarayana, S., 2000. Preparation and characterization of amyloglucosidase adsorbed on activated charcoal. J. Mol. Catal. B Enzym. 10 (5), 471–476.
Ruan, X., Sun, Y., Du, W., Tang, Y., Liu, Q., Zhang, Z., Doherty, W., Frost, R.L., Qian, G., Tsang, D.C.W., 2019. Formation, characteristics, and applications of environmentally

persistent free radicals in biochars: a review. Bioresour. Technol. 281, 457–468.
Schmitt, J., Flemming, H.-C., 1998. FTIR-spectroscopy in microbial and material analysis. Int. Biodeter. Biodegr. 41 (1), 1–11.
Sun, H., Jin, X., Jiang, F., Zhang, R., 2018. Immobilization of horseradish peroxidase on ZnO nanowires/macroporous SiO2 composites for the complete decolorization of anthraquinone dyes. Biotechnol. Appl. Bioc. 65 (2), 220–229.
Sun, Y., Yu, I.K.M., Tsang, D.C.W., Cao, X., Lin, D., Wang, L., Graham, N.J.D., Alessi, D.S., Komárek, M., Ok, Y.S., Feng, Y., Li, X.-D., 2019. Multifunctional iron-biochar composites for the removal of potentially toxic elements, inherent cations, and hetero-chloride from hydraulic fracturing wastewater. Environ. Int. 124, 521–532.
Wang, F., Guo, C., Liu, H.-Z., Liu, C.-Z., 2007. Reversible immobilization of glucoamylase by metal affinity adsorption on magnetic chelator particles. J. Mol. Catal. B Enzym. 48 (1–2), 1–7.
Wang, F., Guo, C., Liu, H.Z., Liu, C.Z., 2008. Immobilization of Pycnoporus sanguineus laccase by metal affinity adsorption on magnetic chelator particles. J. Chem. Technol. Biot. 83 (1), 97–104.
Wang, F., Guo, C., Yang, L., Liu, C.-Z., 2010. Magnetic mesoporous silica nanoparticles: fabrication and their laccase immobilization performance. Bioresour. Technol. 101 (23), 8931–8935.
Wu, D., Feng, Q., Xu, T., Wei, A., Fong, H., 2018. Electrospun blend nanofiber membrane consisting of polyurethane, amidoxime polyarcylonitrile, and β-cyclodextrin as high-performance carrier/support for efficient and reusable immobilization of laccase. Chem. Eng. J. 331, 517–526.
Ye, S., Yan, M., Tan, X., Liang, J., Zeng, G., Wu, H., Song, B., Zhou, C., Yang, Y., Wang, H., 2019. Facile assembled biochar-based nanocomposite with improved graphitization for efficient photocatalytic activity driven by visible light. Appl. Catal. B Environ. 250, 78–88.
Ye, S., Zeng, G., Wu, H., Zhang, C., Liang, J., Dai, J., Liu, Z., Xiong, W., Wan, J., Xu, P., Cheng, M., 2017. Co-occurrence and interactions of pollutants, and their impacts on soil remediation—a review. Crit. Rev. Env. Sci. Technol. 47 (16), 1528–1553.
Yesilada, O., Birhanli, E., Geckil, H., 2018. Bioremediation and decolorization of textile dyes by white rot fungi and laccase enzymes. Mycoremediation and Environmental Sustainability. Springer, pp. 121–153.
Zang, L., Qiu, J., Wu, X., Zhang, W., Sakai, E., Wei, Y., 2014. Preparation of magnetic chitosan nanoparticles As support for cellulase immobilization. Ind. Eng. Chem. Res. 53 (9), 3448–3454.
Zhang, H., Xue, G., Chen, H., Li, X., 2018. Magnetic biochar catalyst derived from biological sludge and ferric sludge using hydrothermal carbonization: preparation, characterization and its circulation in Fenton process for dyeing wastewater treatment. Chemosphere 191, 64–71.
Zhou, G., Chen, Z., Fang, F., He, Y., Sun, H., Shi, H., 2015. Fenton-like degradation of Methylene Blue using paper mill sludge-derived magnetically separable heterogeneous catalyst: characterization and mechanism. J. Environ. Sci. 35, 20–26.